J. Plasma Physics (1997), *vol.* 58, *part* 3, *pp.* 441–453. Printed in the United Kingdom
© 1997 Cambridge University Press

Intrinsic modulational Alfvénic turbulence

L. P. L. de OLIVEIRA,[1] F. B. RIZZATO[1] and A. C.-L. CHIAN[2]

[1]Instituto de Física, Universidade Federal do Rio Grande do Sul PO Box 15501, 91501-970 Porto Alegre, Rio Grande do Sul Brazil

[2]Instituto Nacional de Pesquisas Espaciais–INPE, PO Box 515, 12227-010 São José dos Campos, São Paulo, Brazil

(Received 10 May 1996 and in revised form 17 February 1997)

The nonlinear dynamics of a finite-amplitude Alfvén wave in a dispersive modulational regime is analysed. Use is made of a conservative model to show that turbulence may arise via deterministic chaos. The behaviour of the system is studied as one varies the initial amplitude of the pump Alfvén wave, the dispersion parameter and the plasma parameter β.

1. Introduction

Alfvén waves seem to provide an important way by which energy propagates in the magnetohydrodynamic (MHD) plasmas, probably because fluctuations of this type do not dissipate easily (Barnes & Hollweg 1974). In space plasmas, for example, the concept of Alfvén waves has been used for understanding a number of processes on MHD scales. In fact, in the solar wind, fluctuations of this type are found to be ubiquitous, and turbulent regimes with high Alfvénicity are observed mainly in the fast wind regimes (Belcher and Davies 1971; Marsch and Tu 1990). In the planetary magnetosphere, both travelling and standing Alfvén-wave patterns have been detected, and are occasionally associated with some ultralow-frequency micropulsations (Fukunishi and Lanzerotti 1989; Knudsen *et al.* 1990). The nonlinear dynamics of Alfvénic fluctuations is believed to be the cause of some of the observed local density depressions and temperature enhancements in the auroral zone (Boehm *et al.* 1990; Chian and de Oliveira 1994; de Oliveira and Chian 1996).

A finite-amplitude Alfvén wave can be coupled parametrically to the local density fluctuations, which, even if initially small, are likely to be amplified and take part in the (nonlinear) dynamics. The nonlinear dynamics of Alfvén waves coupled parametrically to density fluctuations has been treated in many works. Spangler and Sheering (1982), Spangler *et al.* (1985) and Hada *et al.* (1989), among others, have found nonlinear coherent solutions of the *derivative nonlinear Schrödinger* (*DNLS*) equation, which models the quasistatic evolution of an Alfvén wave under a weakly nonlinear and dispersive regime, dispersion coming from the finite-Larmor-radius effect. A variety of nonlinear solutions, such as solitons and periodic elliptic functions, were obtained. Ghosh and Papadopoulos (1987) and Hada *et al.* (1990) found, in dissipative regimes, chaotic (non-coherent) solutions for space-periodic and stationary solutions of the DNLS equation respectively; this is indicative that Alfvénic turbulence can be a consequence of the nonlinearities of the problem. Ovenden *et al.* (1983) used a *soliton-gas model* for a space–time modulational regime,

https://doi.org/10.1017/S0022377897005837 Published online by Cambridge University Press

whose envelope dynamics is governed approximately by a *nonlinear Schrödinger* (*NLS*) equation, to explain some features of the power spectra commonly observed in solar-wind Alfvénic fluctuations. For the same purposes, Dawson and Fontán (1990) used similar ideas for modulational regimes based on the DNLS equation. Basically, these statistical formalisms assume that the overall turbulent fluctuations are a consequence of random distribution functions adopted for the soliton phases.

In all of the studies mentioned above, the turbulent regimes are not intrinsic to the Alfvén-wave dynamics, since some external mechanisms are necessary to trigger the turbulence. In fact, like the NLS, the DNLS equation is known to be integrable (Kaup and Newell 1978) and some extrinsic processes, such as driving and dissipation, are required for turbulent solutions to exist. Similarly, in the soliton-gas models, the stochasticity is added externally to the model via the statistical description of the soliton population.

In the present work, we discuss an *intrinsic* model for modulational Alfvénic turbulence. This model results uniquely from the Hamiltonian dynamics of an Alfvén wave in the same modulational regime studied by Ovenden *et al.* (1983), without the need for any external mechanism such as those mentioned above. We shall show that, in this regime, a finite-amplitude Alfvén wave can exhibit chaotic dynamics with many degrees of freedom, giving rise to a turbulent component of the magnetic fluctuations. The chaotic behaviour results from the component of the normalized ion-density fluctuations ρ that is not *Alfvén-resonant*, i.e. that does not satisfy the relation $\partial_t^2\rho = c_A^2\partial_z^2\rho$, where c_A is the Alfvén speed and z is the longitudinal propagation direction of all (plane) fluctuations considered. In fact, if those fluctuations were Alfvén-resonant, the governing equations would reduce to the integrable model used by Ovenden *et al.* (1983), based in NLS soliton solutions. We point out that the chaotic component of the dynamics that will be shown to exist can justify the randomness adopted for the phase of the solitons in the soliton-gas models.

Besides the importance of Alfvén waves for space physics and astrophysics, the problem considered in this paper may be of some interest in the context of the dynamics of nonlinear dispersive waves in general. In effect, it is known that in many cases such dynamics are modelled by continuous systems for which an infinite (in fact uncountable) number of degrees of freedom (or modes) is available for the partition of energy. In principle, as the dynamics of such a system evolves, a distribution of the available energy among all modes can take place. Such a process is known as *energy equipartition* or *thermalization*. However, Thyagaraja (1979) has proved analytically that for space-periodic solutions of a class of continuous systems, of which the NLS is one, no thermalization occurs. This was in fact confirmed by the numerical studies carried out by Martin and Yuen (1980). The absence of thermalization in a given system has deep consequences for the recurrence of its orbits (see Thyagaraja 1983, and references therein), and will be briefly discussed in the last section. We shall show that the space-periodic solutions of the non-integrable system to be considered here, even if occasionally having a large number of modes, seem to present no thermalization.

The integrable model can actually be accurate when the regime is very week, i.e. when the total energy is small. However, we shall see that, even in the absence of thermalization, chaos is present and grows with the total energy.

This paper is organized as follow. In Sec. 2, the fundamental equations are presented and a low-dimension linear stability study is performed to obtain some ana-

https://doi.org/10.1017/S0022377897005837 Published online by Cambridge University Press

lytical predictions about the behaviour of the degree of turbulence as a function of the relevant parameters. In Sec. 3, the numerical simulations results are presented and the analytical predictions of Sec. 2 are checked. In Sec. 4, a discussion and concluding remarks are given.

2. Basic equations and analytical considerations

Let $\mathbf{b}_\pm \equiv b_x \pm i b_y$ be the perpendicular component of the total magnetic field $\mathbf{B} \equiv \mathbf{B}_0 + \mathbf{b}_\pm$ due to Alfvénic (transverse) oscillations with left (+) and right (−) circular polarization. $\mathbf{B}_0 = B_0\hat{\mathbf{z}}$ is the constant and uniform ambient magnetic field. The fully nonlinear equations governing the ponderomotive coupled dynamics of such a wave with density fluctuations (ion acoustic waves) are (Ovenden *et al.* 1983)

$$\{\partial_t^2 - c_A^2\partial_z\,[(1-\rho)\partial_z]\}\mathbf{b}_\pm + \partial_z\,[v_z\partial_t\mathbf{b}_\pm + d_t(v_z\mathbf{b}_\pm)] \pm i\frac{c_A^2}{\boldsymbol{\Omega}_i}\partial_{zt}^2\,[(1-\rho)\partial_z\mathbf{b}_\pm] = 0, \quad (1)$$

$$(\partial_t^2 - c_S^2\partial_z^2)\rho = \tfrac{1}{2}c_A^2\partial_z^2(|\mathbf{b}_\pm|), \quad (2)$$

$$\partial_t\rho + \partial_z(\rho v_z) = 0, \quad (3)$$

where $c_A \equiv B_0/(\mu_0\rho_0)^{1/2}$, $d_t \equiv \partial_t - v_z\partial_z$ and $\boldsymbol{\Omega}_i$ is the gyrofrequency of the ions. In the above equations, the magnetic field $\mathbf{b}_\pm$ and the density ρ are normalized by B_0 and the local constant average density ρ_0 respectively.

The coupled dynamics outlined above can occur in a space–time modulational regime. In this case, one can separate the corresponding magnetic field $\mathbf{b}_\pm$ into a slow amplitude b and a fast harmonic part, writing

$$\mathbf{b}_\pm \equiv b(z,t)\exp[i(k_0z - \omega_0t)]\hat{\mathbf{e}}_\pm \quad (4)$$

with

$$|\partial_t b| \ll |\omega_0 b|\,, \qquad |\partial_z b| \ll |k_0 b|\,, \quad (5)$$

where the vectors $\hat{\mathbf{e}}_\pm \equiv (\mathbf{x} \pm \mathbf{y})/\sqrt{2}$ correspond to left (−) and right (+) circular polarizations. ω_0 and k_0 are the frequency and the wavenumber of the Alfvén wave, which, at $t = 0$, has its maximum amplitude and henceforth will be referred as the *pump*. Then, b represents the envelope of the magnetic oscillations, whose dynamics is governed by the parametric couplings with the density fluctuations ρ. If the approximation $\partial_t^2\rho \approx c_A^2\partial_z^2\rho$ is used to simplify only the nonlinear coupling terms (1)–(3) yield the following non-dimensional equations for the slow components b and ρ:

$$(\partial_t + \partial_z + i\mathcal{P}\alpha\partial_z^2)b = -i\rho b, \quad (6)$$

$$(\partial_t^2 - \beta\partial_z^2)\rho = \beta\partial_z^2(|b|^2), \quad (7)$$

where the normalizations $t \to \omega_0 t$, $z \to k_0 z$ and $b \to 2\beta^{-1/2}b$, with $\beta \equiv c_S^2/c_A^2$, have been adopted. The coefficient $\alpha \equiv (2\boldsymbol{\Omega}_i)^{-1} \ll 1$ represents the weak dispersion due to the finite-Larmor-radius effect, and $\mathcal{P} \equiv \pm 1$ is a polarization identifier, being +1 (−1) for left (right) circular polarizations. The above equations govern the dynamics of the envelope b in a weakly nonlinear and dispersive modulational regime, and are analogous to the Zakharov equations, which are used in the study of modulational dynamics of Langmuir waves (see e.g. Nicholson 1983). In this paper, we are going to be interested in the space-periodic solutions of (6) and (7). Note that the Alfvén-resonant approximation is not used in the linear propagator for the ion-acoustic

https://doi.org/10.1017/S0022377897005837 Published online by Cambridge University Press

waves, the left-hand side of (7), but only in the nonlinear coupling terms. If that resonant approximation had been used, the system would have been reduced to the following NLS-like equation:

$$\partial_t b + \partial_z b + i\mathcal{P}\alpha\partial_z^2 b = -i\mu\,|b|^2\, b, \tag{8}$$

where $\mu = \beta/(1-\beta)$.

In analogy with the Zakharov equations, the system (6), (7) can be expressed in Hamiltonian form (Gibbons *et al.* 1977). Introducing the variable u, defined by $\partial_t u = \rho + |b|^2$, one can rewrite the system as

$$(\partial_t + \partial_z + i\mathcal{P}\alpha\partial_z^2)b = -i\rho b, \tag{9}$$

$$\partial_t u = \rho + b^2, \tag{10}$$

$$\partial_t \rho = \beta\partial_{zz} u. \tag{11}$$

It is now easy to see that the variables b and $f \equiv \frac{1}{2}ib^*$, and ρ and u are canonically conjugate under the Hamiltonian H, whose density is defined by

$$\mathcal{H} = i\alpha(\partial_z b\,\partial_z f - \partial_z b^*\partial_z f^*) - i\rho(bf - b^* f^*) + \tfrac{1}{2}(\rho^2 + \beta\partial_z u^2) \\ -\tfrac{1}{2}\left[(f\partial_z b - b\partial_z f) - (f^*\partial_z b^* - b^*\partial_z f^*)\right], \tag{12}$$

i.e. Hamilton's equations for continuous systems,

$$\partial_t b = \frac{\delta H}{\delta f}, \qquad \partial_t f = \frac{-\delta H}{\delta b},$$

$$\partial_t u = \frac{\delta H}{\delta \rho}, \qquad \partial_t \rho = \frac{-\delta H}{\delta u}$$

are satisfied, where the functional derivatives are calculated as, for instance

$$\frac{\delta H}{\delta b} \equiv \frac{\partial \mathcal{H}}{\partial b} - \frac{\partial}{\partial z}\frac{\partial \mathcal{H}}{\partial(\partial_z b)}$$

(Goldstein 1980)

Again in analogy with the Zakharov equations, our system has the following three constants of motion for space-periodic solutions of period $2L$: the energy

$$H = \int_{-L}^{L} \mathcal{H}\, dz, \tag{13}$$

the action

$$I = \int_{-L}^{L} |b|^2\, dz \tag{14}$$

and the linear momentum

$$P = \int_{-L}^{L} \left[i(b\partial_z b^* - b^*\partial_z b) - \rho\partial_z u\right] dz. \tag{15}$$

These constants will be useful for the verification of the numerical simulations. On the other hand, when the Alfvén-resonant approximation is fulfilled, our system reduces to the NLS equation (8), for which

$$J = -\int_{-L}^{L} |\partial_z b|^2\, dz + \gamma\int_{-L}^{L} |b|^4\, dz, \tag{16}$$

https://doi.org/10.1017/S0022377897005837 Published online by Cambridge University Press

with $\gamma = \beta/[2\alpha(1-\beta)]$, is a constant. As soon as the Alfvén-resonant approximation fails, the constancy of J is broken.

In what follows, we consider the existence of chaotic solutions for the above equations. Such solutions might be typical, given the analogy with the Zakharov equations, which are known to exhibit chaotic behaviour (de Oliveira *et al.* 1995; de Oliveira and Rizzato 1996). In pursuing this goal, we follow de Oliveira *et al.* (1996) and Ghosh and Papadopoulos (1987) in considering space-periodic solutions of (6) and (7), and simulate the propagation of a pump Alfvén wave b_0 of wavenumber and frequency (k_0,ω_0) and initial amplitude parameter $|b_0| \equiv A^{1/2}$. Note that, from the normalization adopted for b, the conventionally normalized amplitude parameter $A_r \equiv |b_{\text{dimensional}}|^2/B_0^2$ is related to A by $A_r = 4\beta A$. Equations (6) and (7) are invariant under the rescaling $t \to \sigma t$, $z \to \sigma z$, $\alpha \to \sigma^{-1}\alpha$, $\rho \to \sigma^{-1}\rho$ and $b \to \sigma^{-1/2}b$, where σ is an arbitrary positive rescaling constant. Under these transformations, those equations remain in exactly the same form, which implies that each set of assumed values for the control parameters in fact represents a family of cases.

In order to obtain some analytical predictions about the degree to which the system (6), (7) exhibits turbulent solutions, we truncate b and ρ to a few Fourier modes, $b \equiv b_0(t)+b_-(t)e^{-ikz}+b_+(t)e^{ikz}$ and $\rho \equiv \rho_1(t)e^{ikz}+\rho_2(t)e^{i2kz}$ with $k \ll 1$, and perform a linear stability analysis for the pump b_0. Assuming that $|b_-|, |b_+|, |\rho_1|, |\rho_2| \ll |b_0|$ and writing $\rho_{1,2} \propto e^{i\omega t}$, linearization of the system of the equations about b_0 yields the dispersion relation

$$[(\omega-k)^2 - \alpha^2 k^4](\omega^2 - \beta k^2) = -2\mathcal{P}\alpha\beta k^4 A. \tag{17}$$

Note that the dispersion effect is essential for the modulational regime considered here since otherwise the frequency ω would always be real and no variation in the amplitudes of the waves involved in the dynamics would occur. The above dispersion relation then describes a modulational instability where the two sidebands corresponding to the linear dispersion relations $\omega = k \pm \alpha k^2$ are lead to grow to generate a modulational envelope (Sakai and Sonnerup 1983; Longtin and Sonnerup 1986). From now on, we shall adopt $\mathcal{P} = 1$, which corresponds to the case where a left-hand polarized wave is unstable when $\beta < 1$. The case $\mathcal{P} = -1$ would correspond to a symmetric situation where a right-hand polarized wave is modulationally unstable if $\beta > 1$.

For the cases where the growth rate $\Gamma^2 \ll k^2(1-\beta)$, we get the simple form

$$\Gamma \approx \left[-\alpha k^2\left(\alpha k^2 - \frac{2\beta A}{1-\beta}\right)\right]^{1/2}, \tag{18}$$

from which we see that the system is unstable if the condition

$$k < k_I \equiv \left[\frac{2\beta A}{\alpha(1-\beta)}\right]^{1/2} \tag{19}$$

is satisfied. So, the number of magnetic modes interacting with the pump at the beginning of the dynamics is given by $N_I \equiv k_I/k$. For a set of parameters like $A_r \approx 0.25$, $\beta \geqslant 0.1$, $\alpha \approx 0.05$, typical of the solar wind, and $k \leqslant 0.1$, one has $k_I \approx 0.454$, which means that there are about $N_I \geqslant 4$ relevant magnetic modes taking part in the dynamics. Note that, under the above-mentioned rescalings, one finds equivalent results where $k_I \to \sigma^{-1}k_I$ and $\Gamma \to \sigma^{-1}\Gamma$, but the number of relevant modes N_I remains the same, $N_I \to N_I$. Since, in this case, $k \ll 1$, we

https://doi.org/10.1017/S0022377897005837 Published online by Cambridge University Press

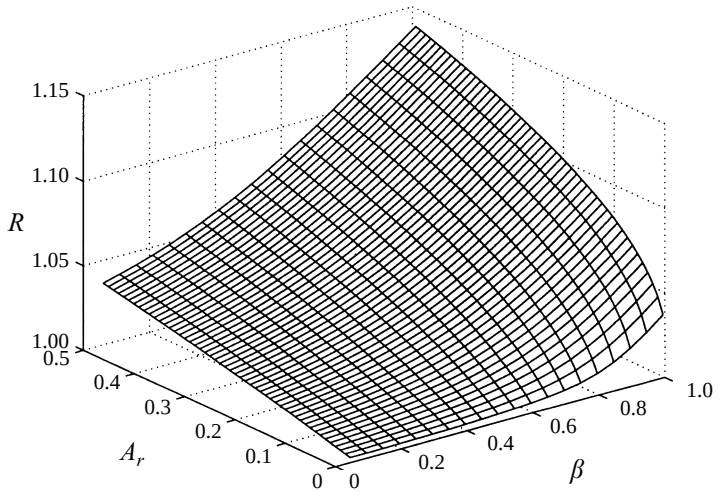


Figure 1. Behaviour of R as a function of the parameters A_r and $\beta < 1$.

expect that the regime can be indeed described relatively well by our modulational approximation.

We now define the parameter $R \equiv |\omega|/|k|$, which measures the validity of the Alfvén-resonant approximation, since the smaller the value of the difference $R-1$, the more valid is that approximation; recall that in our normalized system, the Alfvén-wave velocity is $c_A = 1$. Thus R is a measure of how far from integrability is the system (6), (7) at the beginning of the process. From (18) and $\alpha^2 k^2 \ll 1$, we find

$$R \approx \frac{|k + i\Gamma|}{|k|} \approx \left(1 + \frac{2\alpha\beta A}{1-\beta}\right)^{1/2}, \tag{20}$$

from which we can anticipate that the non-integrable component of (6) and (7) becomes more significant when the pump intensity A_r increases and when $\beta \to 1$, but is practically independent of the value of k. This can also be seen from the numerical solutions of (17) for different values of A_r (or A, for fixed β) and $\beta < 1$, as shown in Fig. 1. Moreover, from (20) and from Fig. 1, we can expect that non-integrability depends more strongly on β variations, when $\beta \to 1$, than on A variations. Like N_I, the quantity R is also invariant with respect to the referred rescaling rules, $R \to R$.

We can also from figure 1 see that at the beginning of the dynamics, our system is not very far from the integrable regime, represented by the NLS equation (8). So, we expect that the constant J does not vary too much, at least for some time after the beginning of the dynamics. This gives us a nonlinear way to estimate the number of effective modes in contrast to the linear estimates represented by N_I we made before. In fact, defining

$$Q \equiv \frac{\int_{-L}^{L} |\partial_z b|^2 \, dz}{I} = \frac{k^2 \sum_{n=-\infty}^{\infty} n^2 |b_n|^2}{\sum_{n=-\infty}^{\infty} |b_n|^2}, \tag{21}$$

and following Thyagaraja (1979), we see that $N_{rms} = Q^{1/2}/k$ is the root mean

https://doi.org/10.1017/S0022377897005837 Published online by Cambridge University Press

square of the number of magnetic modes b_n, where the statistical weights are the intensities $|b_n|^2$. Thyagaraja showed that, for systems preserving I and J, $Q \leqslant M^2$, where, for our case,

$$M = \frac{\gamma}{2} I + \frac{1}{2} \left[\gamma^2 I^2 + 4 \left(\frac{J}{I} + \frac{\gamma}{2} I \right) \right]^{1/2}. \tag{22}$$

So, considering pump-like initial conditions, we can calculate the values of I and J and finally obtain estimates for Q and N_{rms}. For the interesting cases, we have $\alpha k/\beta \ll 1$, and so, carring out the above procedure, we get

$$N_{rms} \approx \frac{\pi A \beta}{\alpha k^2 (1 - \beta)} = \tfrac{1}{2} \pi N_I^2. \tag{23}$$

While N_I gives an estimate of the minimum, N_{rms} gives a estimate of the maximum number of effective modes taking part in the dynamics, above which energy redistribution is arrested. As we shall see, this is confirmed by the numerical simulations. Note that, according to (23), the qualitative dependences of N_I and N_{rms} on the parameters A, β and α are similar, except for the square root.

So far, our results show that, even at the onset of the coupled dynamics, a non-integrable component of the envelope dynamics does exist, which is induced by ion-acoustic oscillations off Alfvén resonance. It is also argued that the class of solutions considered displays a large number of effective modes but no thermalization. In fact, in the next section, we shall show that chaotic regimes exist, and that both the degree of temporal stochasticity and the number of active modes depend on the parameters A, β and α in a manner that is consistent with our analytically estimated predictions, based on R and N_I. The absence of thermalization will also be verified.

3. Numerical simulations

For space-periodic solutions of (6) and (7), we proceed to numerical simulations using a spectral method (Tajima 1989), which consists in expressing the magnetic field b and the density oscillations ρ as Fourier series

$$f(z,t) = \sum_{n=-N/2}^{(N-2)/2} f_n(t) \exp(inkz), \tag{24}$$

where f represents b or ρ, and integrating the resulting set of ordinary differential equations (ODEs) for the Fourier coefficients $b_n(t)$ and $\rho_n(t)$. We used Runge–Kutta and predictor–corrector routines for the ODE integrations, and the number of modes N was varied between 128 or 256, depending on the convergence and consistency requirements for the different A, β and α values. The nonlinear coupling terms are fast-Fourier-inverted in order to calculate the products in real space, and the result is then fast-Fourier-transformed back to the ODEs. The numerical values of the constants H, I and P are calculated, in order to verify the accuracy of the numerical simulations. Accuracies of $1 : 10^8$ are obtained.

In general, our dynamics exhibit complexity in space and time. Temporal complexity is in principle measured in terms of sensitivity to initial conditions and associated with a series of positive Lyapunov exponents $\lambda_1 \geqslant \lambda_2 \geqslant \ldots \geqslant \lambda_p \geqslant 0$. However, as time passes, the *main Lyapunov exponent* λ_1 dominates the others and

https://doi.org/10.1017/S0022377897005837 Published online by Cambridge University Press

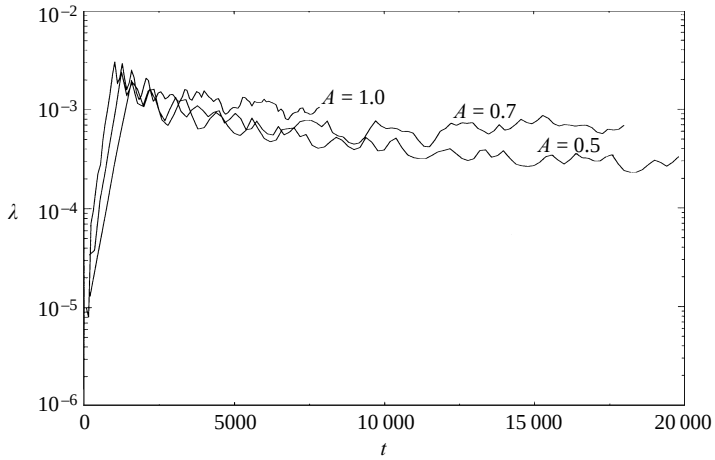


Figure 2. Convergence of the partial Lyapunov exponents for $A = 0.5$, 0.7 and 1.0. The asymptotic values correspond to the main Lyapunov exponent for each case. The others parameters are kept fixed as $\alpha = 0.05$, $\beta = 0.01$ and $k = 0.1$.

can be taken itself as a measure of sensitivity to initial conditions (Lichtenberg and Lieberman 1983). A temporally complex dynamics, also known as chaotic, does not necessarily involve a large number of unstable modes. But if it does, we shall loosely speak of it as revealing space–time complexity, or turbulence.

To calculate the main Lyapunov exponent λ_1, we use the method developed by Benettin *et al.* (1976) (Lichtenberg and Lieberman 1983). This method consists in calculating partial Lyapunov exponents $\lambda(t)$, which converge asymptotically to the λ_1 value, i.e. $\lambda_1 = \lim_{t\to\infty} \lambda(t)$. Figure 2 shows the main Lyapunov exponent λ_1 calculated for different values of the parameter A: $A = 0.5$, $A = 0.7$ and $A = 1.0$. The other parameters are fixed at $k = 0.1$, $\beta = 0.01$ and $\alpha = 0.05$. In accordance with the results of the previous section, chaotic activity increases with A (and A_r). In fact one can see that for increasing values of A, the Lyapunov exponents are 3×10^{-4}, 7×10^{-4} and 10^{-3}, respectively. This is a consequence of the ion-acoustic fluctuations, which are not Alfvén-resonant, as was signalled by the parameter $R \neq 1$. This behaviour can be thought as natural, since the growth rate Γ associated with the dynamics also grows with A, and therefore the nonlinear interactions between the Fourier modes become more intense.

Figure 3 displays the partial Lyapunov exponents for some values of the parameter β. For $\beta = 0.07$, the partial exponents converge to $\lambda_1 = 10^{-3}$, while for $\beta = 0.22$ and $\beta = 0.49$, they converge to $\lambda_1 = 2.3 \times 10^{-3}$ and $\lambda_1 = 2 \times 10^{-2}$ respectively. The other parameters are fixed as $k = 0.025$ and $\alpha = 0.2$, except A, which is normalized by 2β and varies in a way such that $A_r = \sqrt{2}/40$ is kept fixed. Again in accordance with the results of the previous section, λ_1 grows with $\beta < 1$. Note that, on comparing Figs 2 and 3, one can see that λ_1 is more sensitive to β variations than to A variations. In fact, one sees from Fig. 2 that the Lyapunov exponent λ_1 found for $A = 1.0$ is about 3.3 times larger than that found for $A = 0.5$, while one observes from Fig. 3 that the λ_1 value found for $\beta = 0.49$ is about 15 times larger than that found for $\beta = 0.22$, which is almost half of the first value. This is also consistent with the conclusions drawn in the previous section.

In the simulations, we assume, as initial conditions, Fourier-mode amplitudes

https://doi.org/10.1017/S0022377897005837 Published online by Cambridge University Press

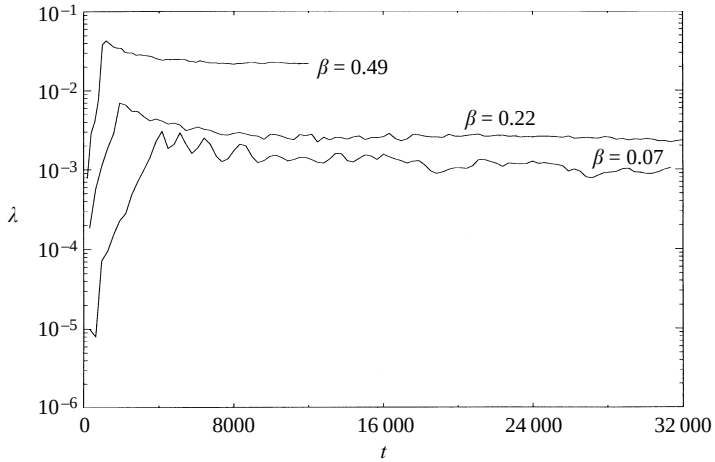


Figure 3. Convergence of the partial Lyapunov exponents for some values of β: $\beta = 0.07$, 0.22 and 0.49. The other parameters are fixed as $\alpha = 0.2$, $k = 0.025$ and $A_r = \sqrt{2}/40$.

such that b satisfies $|b_0/b_{\pm 1}| = 100$. The remaining involved modes, including those corresponding to ρ and its derivative, are assumed to be numerically null. However, even if initially sharp, the spectral bandwidth becomes larger and larger as time evolves, until a saturated bandwidth limit is attained; no thermalization is verified in any case. In order to illustrate this and check the conclusions about the dependence of the number of relevant modes on the parameters A, β and α, Fig. 4 displays the spectral intensity for different sets of parameter values, at the beginning (thin lines) and as typically obtained at the end of the respective simulations (thick lines). It is easy to see from this figure that the bandwidth increases as A grows (a, b), as α decreases (b, c), and as β grows, approaching 1. The estimates based on N_I have been shown to be more accurate than those based on the constant M, as proposed by Thyagaraja. In fact, similarly to Martin and Yuen (1980), in our numerical experiments, Thyagaraja's bounds have given values for N_{rms} much greater than those verified in the numerical results. On the other hand, the estimates based on N_I give better results for both absolute and r.m.s. number of modes, as one can check from Figs 4 and 5.

It is interesting to note that the case illustrated in Fig. 5 is the farthest from the integrable NLS regime among all the situations studied. In fact, it corresponds to the highest Lyapunov exponent obtained in the numerical simulations, and accordingly to the highest R value, as one can see from Fig. 1. This suggests that, in all cases treated here, we have no thermalization, owing to the quasi-constancy of J.

Our simulations therefore confirm the simple analytical predictions of the previous section about the behaviour of the turbulence level of the solutions with respect to the parameters A and β. We could not obtain clear results about the Lyapunov exponent as a function of α, since the range of values for which we could perform meaningful simulations was restricted. As we attempt to compare the present results with results for smaller values of the dispersion, the number of modes increases and the simulation becomes prohibitively time-consuming. On the other hand, larger dispersion does not fulfil the weak dispersion condition.

https://doi.org/10.1017/S0022377897005837 Published online by Cambridge University Press

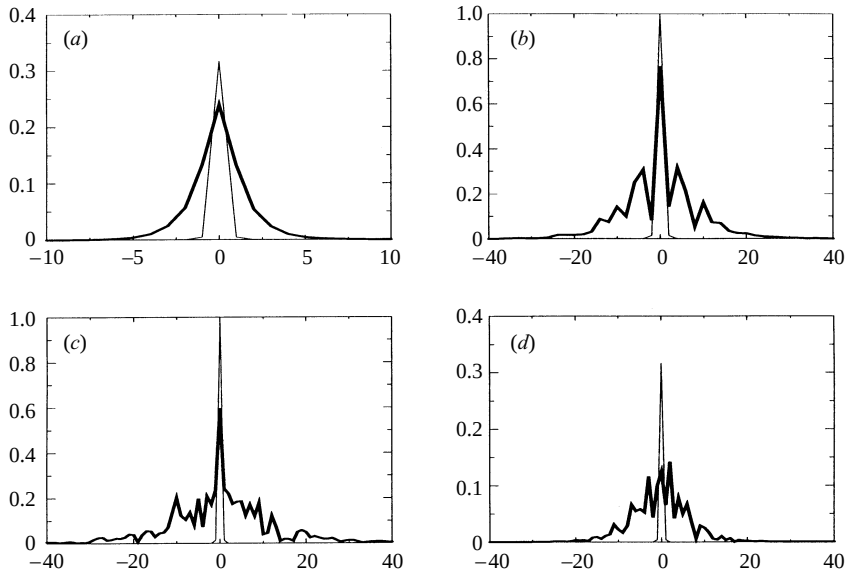


Figure 4. Spectral intensities ($|b|$ versus n) obtained by the end of the simulations (thick lines) for the following sets of parameter values: (*a*) $A = 0.1$, $\beta = 0.01$, $\alpha = 0.05$, $k = 0.1$; (*b*) $A = 1.0$, $\beta = 0.01$, $\alpha = 0.05$, $k = 0.1$; (*c*) $A = 1.0$, $\beta = 0.01$, $\alpha = 0.01$, $k = 0.1$. (*d*) $A_r = 0.14$, $\beta = 0.1$, $\alpha = 0.05$, $k = 0.1$. The initial spectra are represented by the thin lines.

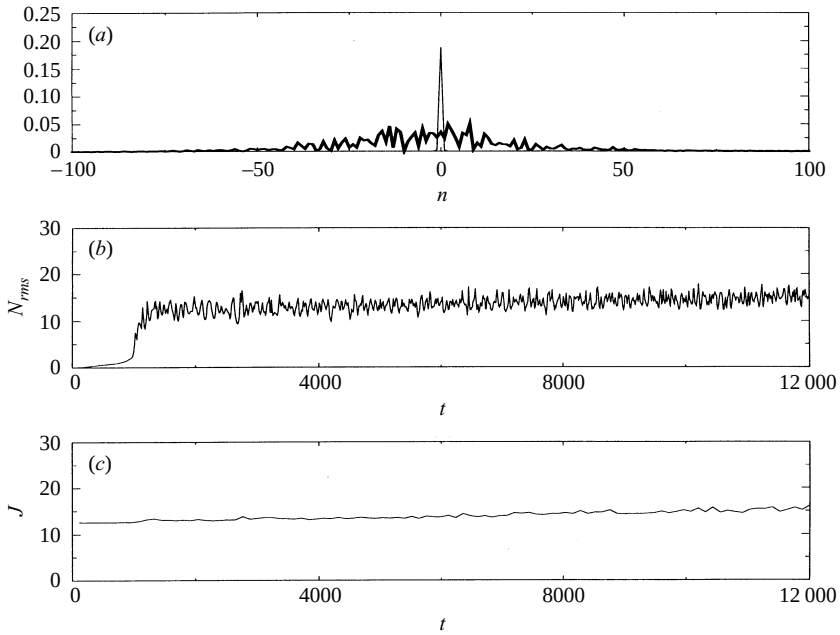


Figure 5. (*a*) Spectral intensities (as in Fig. 4), (*b*) N_{rms} and (*c*) J, obtained from numerical simulation with $A_r = \sqrt{2}/40$, $\beta = 0.49$, $\alpha = 0.2$ and $k = 0.025$ (see Fig. 3).

https://doi.org/10.1017/S0022377897005837 Published online by Cambridge University Press

4. Discussion and concluding remarks

In this paper, we have shown that the dynamics of Alfvén waves, in the dispersive modulational regime considered, can be intrinsically turbulent. Accordingly, we have shown that the dynamics of a finite-amplitude Alfvén wave, with no external driving, like a source or dissipation, can exhibit chaotic dynamics with many degrees of freedom resulting in complex space–time Hamiltonian evolution. In fact, the system (6), (7) represents a perturbation of an NLS equation, which is integrable. The integrability is broken when we consider sets of control parameters A, β and α for which R is different from unity. This allows a significant level of density fluctuations that are not Alfvén-resonant to take part in the dynamics. In this situation, some of the NLS constants of motion, including J, are no longer valid, but vary with time, and chaotic dynamics arises.

The complexity or, alternatively, the level of turbulence depends on the amplitude parameter A, and on the plasma parameters β and α. In fact, one has stronger turbulence for larger A and β (< 1) values, since the number of relevant magnetic modes as well as the main Lyapunov exponent are larger. The role of the parameter α is somewhat different from those of the parameters A and β. In fact, it can be seen from (19) and (20), that, while the parameter R grows with the dispersion parameter α, N_I decreases. This means that, as α grows, the complexity in space is diminished while the complexity in time becomes more significant, and vice versa. Therefore the dispersion resulting from the finite-Larmor-radius effect acts as a regulating mechanism for the number of relevant modes in the considered regime. Dispersion is typically small for MHD settings, so we were limited in taking relatively small values for α. This was why we always had a large (>3) number of relevant magnetic modes in the dynamics found in the feasible numerical simulations. Moreover, when $\alpha > 0$, one always has $\Gamma > 0$ and, from (20), $R > 1$. This means that an Alfvénic off-resonant component of density ρ is always present in the dynamics, thus destroying the integrability of the system (6), (7).

Although the numbers of relevant modes for most of our simulations were relatively high, no thermalization was verified in any case, and only a finite number of the available modes took part in the energy redistribution (Yuen and Fergusson 1978; Martin and Yuen 1980). According to Poincaré's theorem, we conclude that, although chaotic, our system displays recurrence (see Thyagaraja 1983, and references therein). In fact, Thyagaraja's arguments are based fundamentally on the constancy of I and J, as happens, for example, for the NLS equation. In the present case, I continues to be conserved, while J, even if not constant, is almost conserved, since our system is a perturbation of an NLS. This is illustrated in Fig. 5, where results for the most non-integrable case treated in this work are displayed.

According to our studies, one can identify two classes of nonlinear regimes. In the weakly nonlinear regimes, one has values for A, β, α and k giving a modulational regime where $N_I k \ll 1$; we have focused the present analysis on this case. Conversely, in strongly nonlinear regimes, the condition on $N_I k$ is not satisfied, and the envelope energy is progressively transferred to smaller scales comparable to the carrier space–time scale. In this case, all the available modulational scales are energized, and the modulational approximations should not be expected to provide an accurate description of the wave dynamics. For practical applications, depending on the A, β, α and k values, this transfer of energy can take place in a rather short time compared with the time necessary for the chaotic process to develop fully. In

https://doi.org/10.1017/S0022377897005837 Published online by Cambridge University Press

these cases, the NLS regular solutions should provide a rather good description of the dynamics for the short period while the energy is still restricted to the modulational scales. The lifetime of such solutions, however, is short, and moves away from the modulational scales. The transition from the weakly to the strongly nonlinear regime will be reported elsewhere.

The results of our studies can have some implications in understanding the presence of solitons and turbulence in the solar wind, as proposed by Ovenden *et al.* (1983). In fact, all the parameter values considered in our simulations are somewhat typical of that kind of environment, except for β, whose values are slightly smaller than the most typical values, which are closer to unity. This suggests that a modulational turbulent regime can be even more intense there. According to our studies, a modulational soliton turbulence regime such as that proposed by Ovenden *et al.* (1983) would belong to the class of strongly nonlinear regimes.

To conclude, our analysis shows that for typical system parameters, one is likely to observe non-integrable features that arise from the ion-acoustic equation. In fact, owing to the multitude of degrees of freedom typically found here and the known intrinsic instability of multifrequency systems, one cannot expect the integrable model to provide a very faithful description of the system.

Acknowledgements

The authors acknowledge partial support from Conselho Nacional de Desenvolvimento Científico e Tecnológico (CNPq–Brazil) and from Fundação de Amparo à Pesquisa do Rio Grande do Sul (FAPERGS–RS–BR). Numerical calculations were performed on the Cray Y-MP2E at the Universidade Federal do Rio Grande do Sul Supercomputing Centre. Finally, the authors are grateful for the suggestions of the referees.

References

Belcher, J. W. and Davies L. 1971, *J. Geophys. Res.* **76**, 3534.

Benettin, G., Galgani, L. and Strelcyn, J. M. 1976 *Phys. Rev.* **A14**, 2338.

Boehm M. H., Carlson C. W., McFadden J. P., Clemmons J. H. and Mozer F. S. 1990, *J. Geophys. Res.* **95**, 12157.

Chian A. C.-L. and de Oliveira, L. P. L. 1994 *Astron. Astrophys.*, **286**, L1-L4.

Dawson, S. P. and Fontán, C. F. 1990 *Astrophys. J.* **348**, 761.

de Oliveira, L. P. L. and Chian, A. C.-L 1996 *J. Plasma Phys.* **56**, 251.

de Oliveira, G. I. and Rizzato, F. B. 1996 *Phys. Lett.* **214A**, 40.

de Oliveira, G. I., Rizzato, F. B. and Chian, A. C.-L. 1995 *Phys. Rev.* **E52**, 2025.

de Oliveira, G. I., de Oliveira, L. P. L. and Rizzato, F. B. 1996, *Phys. Rev.* **E54**, 3239.

Fukunishi, H. and Lanzerotti, L. J. 1989 *Plasma Waves and Instabilities at Comets and in Magnetospheres* (ed. B. J. Tsurutani and H. Oya), p. 179. American Geophysical Union, Washington, DC.

Ghosh, S. and Papadopoulos, K. 1987 *Phys. Fluids* **30**, 1371.

Gibbons, J., Thornhill, S. G., Wardrop, M. J. and ter Haar, D. 1977 *J. Plasma Phys.* **17**, 153.

Goldstein, H. 1980 *Classical Mechanics*, 2nd edn. Addison-Wesley, Reading, MA.

Hada, T., Kennel, C. F. and Buti, B. 1989 *J. Geophys. Res.* **94**, 65.

Hada, T., Kennel, C. F., Buti, B. and Mjølhus, E. 1990 *Phys. Fluids* **B2**, 2581.

Kaup, D. J. and Newell, A. C. 1978 *J. Math. Phys.* **19**, 798.

Knudsen, D. J., Kelley, M. C., Earle, G. D., Vickrey, J. F. and Boehm, M. 1990, *Geophys. Res. Lett.* **17**, 921.

https://doi.org/10.1017/S0022377897005837 Published online by Cambridge University Press

Lichtenberg, A. J. and Lieberman, M. J. 1983 *Regular and Stochastic Motions*. Springer-Verlag, New York.
Longtin, M. and Sonnerup, B. U. Ö. 1986 *J. Geophys. Res.* **91**, 6816.
Marsch, E. and Tu, C.-Y. 1990 *J. Geophys. Res.* **95**, 8211.
Martin, D. U. and Yuen, H. C. 1980 *Phys. Fluids* **23**, 1269.
Nicholson, D. R. 1983 *Introduction to Plasma Theory*. Wiley, New York.
Ovenden, C. R., Shah, H. A. and Schwartz, S. J. 1983 *J. Geophys. Res.* **88**, 6095.
Sakai, J.-I. and Sonnerup, B. U. Ö., 1983 *J. Geophys. Res.* **88**, 9069.
Spangler, S. R. and Sheerin, J. P. 1982 *J. Plasma Phys.* **27**, 193.
Spangler, S. R., Sheerin, J. P. and Payne, L. 1985 *Phys. Fluids* **28**, 104.
Tajima, T. 1989 *Computational Plasma Physics: With Applications to Fusion and Astrophysics*. Addison-Wesley, Reading, MA.
Thyagaraja, A. 1979 *Phys. Fluids* **22**, 2093.
Thyagaraja, A. 1983 *Nonlinear Waves* (ed. L. Debnath), p. 308. Cambridge University Press.
Yuen, H. C. and Fergusson, W. E. 1978 *Phys. Fluids* **21**, 1275.

https://doi.org/10.1017/S0022377897005837 Published online by Cambridge University Press